

ROTOR DYNAMIC BEHAVIOUR OF A HIGH-SPEED OIL-FREE MOTOR COMPRESSOR WITH
A RIGID COUPLING SUPPORTED ON FOUR RADIAL MAGNETIC BEARINGS

J. Schmied
Sulzer Escher Wyss
Zurich, Switzerland

59-37

11917

2-16

J.C. Pradetto
Sulzer Escher Wyss
Zurich, Switzerland

SUMMARY

The combination of a high-speed motor, dry gas seals and magnetic bearings realized in this unit facilitates the elimination of oil. The motor is coupled with a quill shaft to the compressor. This yields higher natural frequencies of the rotor than with the use of a diaphragm coupling and helps to maintain a sufficient margin of the maximum speed to the frequency of the second compressor bending mode. However, the controller of each bearing then has to take the combined modes of both machines into account. The requirements for the controller to ensure stability and sufficient damping of all critical speeds are described and compared with the implemented controller. The calculated closed loop behaviour was confirmed experimentally, except the stability of some higher modes due to slight frequency deviations of the rotor model to the actual rotor. The influence of a mechanical damper as a device to provide additional damping to high modes is demonstrated theoretically. After all, it was not necessary to install the damper, since all modes could be stabilized by the controller.

INTRODUCTION

The task of the motor compressor unit is to fill a cavern with natural gas for storage purposes. A compressor without any oil is desirable for this application, since the smallest quantities of oil in the gas cause considerable additional maintenance costs for the pipes. The elimination of any oil could be realized by the combination of a high-speed motor (no gear necessary), dry gas seals replacing oil seals and magnetic bearings substituting oil bearings. Figure 1 shows a cross section of the compressor and Figure 2 the whole unit. The motor is located in a separate housing. Its shaft is connected to the compressor shaft with a quill shaft.

The suction pressure of the compressor is 50 bar and the maximum discharge pressure is 150 bar. The maximum output of the motor is 2MW and the operating speed ranges from 14000 rpm to 20000 rpm.

The discharge pressure of the compressor at the drive end is sealed against atmospheric pressure with a triple dry gas seal. The helium cooling gas of the motor at the drive end is also sealed with a dry gas seal. The thrust bearing and the radial bearing on the non drive end side are surrounded by the natural gas working fluid, but at a lower pressure than suction pressure in order to reduce windage losses. This requires another seal between the first compressor stage and the thrust bearing.

Due to the high efficiency requirements, the compressor does not have a balance piston with its relevant high leakage losses. The thrust is balanced by a digital valve controlling the flow into a chamber at the non drive end of the compressor as a function of the flux of the magnetic thrust bearing, which is proportional to the thrust force. The resulting pressure in the balance chamber is also sealed with a dry gas seal.

The main object of the paper is to describe the predicted and measured rotordynamic behaviour of this unit and its influence on the design of the digital controller, with special regard to the aspects of the quill shaft coupling. In comparison with a diaphragm coupling, this type of coupling offers several advantages:

- Less weight (yields higher natural frequencies),
- additional stiffness (yields higher natural frequencies),
- high reliability (the possibility of diaphragm cracks is eliminated),
- requirement of only one bearing to take the thrust.

The main reason for the choice of the quill shaft is the higher natural frequencies of the rotor yielding a greater margin of the maximum speed to the second bending mode frequency of the compressor. However, because of this type of coupling the alignment of the compressor had to be handled very carefully, since it changes the bearing loads, and the controller of each bearing had to account for the combined modes of both rotors (compressor and motor).

DESCRIPTION OF THE ROTOR AND ITS DYNAMIC BEHAVIOUR

The basic data of the two shafts connected with a quill shaft are as follows:

Weight of the motor shaft:	240 kg.
Weight of the compressor shaft:	100 kg.
Length of the motor shaft:	app. 1.1 m.
Length of the compressor shaft:	app. 1.2 m.
Frequency of the first bending mode (motor alone in free condition):	440 Hz.
Frequency of the first bending mode (compressor alone in free condition):	220 Hz.

The connecting quill shaft has a length of 285mm and a diameter of 30mm.

Figure 3 shows the modes of the connected shafts at standstill and supported on soft springs. The vertical lines indicate the sensor (outer lines) and actuator positions (inner lines). It can be seen that each mode shape exhibits dominating deflections in one of the two rotors; hence they can be classified almost as the modes of the single rotors. However, every mode also has slight deflections in the other rotor.

Table 1 shows the observability (sensor not in a node) and commandability (actuator not in a node) of each mode. All modes below the maximum speed (up to the fifth) should be readily observable and commandable in order to enable the bearings to provide sufficient damping. Higher modes need not be well damped, but they must not be excited by the bearings. Good observability and commandability of these modes are not necessary, and in some cases not desirable either.

Figure 4 shows the natural frequencies of the modes at standstill and at full speed. It shows how the frequencies are shifted by the gyroscopic effect. The frequencies of the modes above the fourth are not shifted by more than 5%. The magnetic bearing controllers must be insensitive to these shifts.

REQUIRED AND REALIZED BEARING TRANSFER FUNCTION

The transfer function of the magnetic bearing (= relation between input (=sensor displacement signal) and output (= bearing force)) is mainly determined by the controller. Hence designing the transfer function means tuning the controller.

Figures 5,6 and 7 show the realized transfer functions (amplitude and phase) for the motor and compressor bearings. They also include an approximation for the amplifier and actuator. The motor bearing function has the order 12 in the z domain, those of the two compressor bearings 13. The relationship between amplitude and phase of the transfer function and stiffness and damping of the bearing is given by the following formulae.

$$A = \sqrt{(d\omega)^2 + k^2} \quad (1)$$

$$\phi = \arctan (d\omega/k) \quad (2)$$

or

$$k = A \cos \phi \quad (3)$$

$$d = A \sin \phi / \omega \quad (4)$$

An analysis of the compressor rotor was carried out with two similar bearings having a spring and damper characteristic in order to get an idea in the design phase of the necessary bearing damping for a sufficient damping ratio of all modes below the maximum speed. The noncollocation of sensor and actuator is taken into account as described in /1/ and /2/. The analysis was carried out for the compressor only, because its bending mode is in the operating speed range.

Figures 8 and 9 show the eigenvalues (damping ratio and frequency) of the first three compressor modes for two bearing stiffnesses (10^7 N/m and $2 \cdot 10^7$ N/m) and various bearing damping coefficients. The stiffness should not be lower than 10^7 N/m in order to enable the bearing to withstand aerodynamic excitations. On the other hand, it should not be much higher because the bearing damping then becomes less efficient. A damping ratio of 10% is normally the minimum requirement for safe operation in the critical speed, although much higher damping ratios are possible.

Table 2 shows a comparison of the realized and necessary characteristics needed to damp the compressor bending mode according to the minimum requirement of 10%. It is not fulfilled on the drive

end side, whereas it is surpassed on the non drive side. An analysis of the eigenvalues of the closed loop system will show whether the combination can fulfil the requirement.

The modes above the maximum speed, which must not be excited by the bearings, are the reason that the realized bearing damping is to be of a magnitude equal to the minimum requirement and not much higher. For positive bearing damping, an excitation can happen if the mode shape has a node between sensor and actuator. It can also happen if the bearing damping becomes negative due to phase losses in the actuator and amplifier or due to phase losses caused by the sampling of the digital controller. In order to prevent an excitation a bad observability or commandability of the mode and a low amplitude of the transfer function are helpful. A low amplitude in the high frequency region limits the bearing damping at the bending mode frequency. For the well observable and commandable high modes, the transfer function should provide some damping. This means it should have a phase between either 0° and 90° , or between -180° and -270° . This yields positive damping according to equation (4). The latter case yields a negative stiffness according to equation (3), but is not destabilizing for high modes. The compressor DE bearing can observe and command all modes up to 1500 Hz, most of them well (see table 1). The tuning of this bearing was particularly difficult therefore. An analysis of the eigenvalues will show if all modes are stable in the higher frequency region.

THE CLOSED LOOP BEHAVIOUR

Analysis

All analog parts are transformed to the z domain, duly considering the zero order hold, for the analysis of the closed loop behaviour. The analog parts are the rotor (its finite element model), the sensor and the actuator. These three parts are in series mode at each bearing. The closed loop system with the digital controller can then be built in the z domain. All these operations are carried out with the programme MATLAB. The modeling of the rotor and the plotting of eigenvectors are carried out with the finite element programme MADYN /3/. Figure 10 provides an overview for the procedure of the closed loop calculations.

Results

Figure 11 shows the modes (real and imaginary part, which are the shapes at two instances $\omega t=90^\circ$ apart) of the closed loop system up to 1500 Hz at standstill. The demonstrated modes are only modes with major deflections in the rotor. They correspond to the modes of the rotor supported on soft springs. Due to the controller coordinates, additional modes arise which are not shown here. They are well damped, have relative small rotor deflections and normally are of no practical importance.

Table 3 shows the calculated damping ratios as well as a comparison of the calculated frequencies with measured frequencies. The coincidence of measured and calculated frequencies is not poor up to the seventh mode (second compressor bending mode). There are considerable deviations above this mode.

Two of the modes above the maximum speed (20000 rpm = 33 Hz) are unstable: The eighth and eleventh mode. This is due to the inaccurate frequencies of these modes. Due to the deviation of the calculated frequency, the eighth mode is in a region, where the transfer function of the DE bearing of the compressor has a phase angle of about -150° yielding a negative damping. In reality, the frequency is in a region, where the phase is about -200° yielding a positive damping. The other bearings have only very little or no influence on the stability of this mode. In case of the eleventh mode, the calculated frequency is in a region where the motor bearing transfer function has a phase angle of about -40° , hence a negative damping, whereas in reality the frequency is in a region with positive damping (positive phase angle of about 45°). The compressor bearings have little or no influence on this mode.

The damping ratios for all modes are sufficiently high within the speed range. The first bending mode of the compressor has the lowest damping ratio of these modes. It is 11.8%, which is still above 10%. An unbalance response calculation helps to assess whether this is sufficient to run on the critical speed of this mode.

Figure 12 shows the calculated response of all bearing forces to two parallel unbalances of 60 gmm at the compressor shaft ends. This corresponds to G2.5. The magnetic bearing capacity for dynamic loads is about 600 N. It is reached at the NDE compressor bearing at the critical speed of the bending mode with a balance quality of G1.8, whereas the achieved balance quality is G0.65. An unbalance at the shaft ends is very unfavourable (because it is a very sensitive location) and unlikely to occur in reality. Assuming an unbalance in the middle of the compressor yields even more margin. The permissible unbalance then is more than twice as high. This proved to be sufficient during the extensive test programme of the machine.

EFFECT OF A MECHANICAL DAMPER

Figure 13 shows a sketch of a mechanical damper, which can be mounted on the non drive end side of the compressor. Its purpose is to provide additional damping to the higher modes above the maximum speed. It was prepared as a way out in case the tuning of the magnetic bearing proved unsuccessful. It was not necessary to be installed after all. However, its effect was studied theoretically. For this purpose, the damper was modeled as a concentrated mass (without moments of inertia) attached to the rotor with a spring and damper. The data are as follows:

Mass:	$m = 1.5 \text{ kg}$
Stiffness:	$k = 2.1 \cdot 10^7 \text{ N/m} \Rightarrow f_k = (\sqrt{k/m})/(2\pi) = 600 \text{ Hz}$
Damping ratio (damper alone):	$D = 25\%, 50\%$

Since they were not exactly known two values were assumed for the damping ratio.

Figure 14 shows the effect of the damper on the frequencies and damping ratios of all modes up to 1500 Hz. The high compressor modes 5 to 8 and 10 are affected more than the motor modes 9 and 11. The damping effect on the compressor modes above the damper mode is considerable. The frequencies above the damper mode are increased for a damper damping ratio of 25%, whereas they are slightly decreased as all the others for the 50% case.

CONCLUSIONS

A transfer function of the magnetic bearings was designed which is able to fulfil all necessary requirements: It provides sufficient damping to all modes below maximum speed, especially to the compressor bending mode, which is in the operating speed range and is able to ensure the stability of all modes above maximum speed. This was achieved in spite of a rigid coupling with the consequence, that each bearing has to consider the modes of both rotors. The main advantage of the coupling is a higher margin of the maximum speed to the frequency of the second compressor bending mode. It was not necessary to mount a mechanical damper, which could provide additional damping to the higher modes, as was shown theoretically .

ACKNOWLEDGEMENTS

The authors wish to thank all partners concerned with this project for their excellent cooperation: The magnetic bearing manufacturer S2M in France, the motor manufacturer ACEC in Belgium, the manufacturer of the frequency inverter for the motor, HILL GRAHAMS CONTROL, in England and the seal manufacturer, JOHN CRANE, in England.

REFERENCES

1. Schmied, J.: Experience with Magnetic Bearings Supporting a Pipeline Compressor. Proceedings of the 2nd International Symposium on Magnetic Bearing, July 12-14, 1990, Tokyo, Japan.
2. Schmied, J., Pradetto, J.C.: Selbsterregte Schwingungen bei magnetgelagerten Rotoren. VDI Berichte Nr. 957, 1992.
3. Klement, H.D.: MADYN - Ein Programmsystem für die Maschinenberechnung. Unix/mail 5 (1987).

Table 1. Observability and Commandability of Natural Modes

mode	motor NDE	motor DE	comp. DE	comp. NDE
1, motor parallel	O yes / C yes	O yes / C yes	O weak / C weak	O no / C no
2, comp. parallel	O yes / C yes			
3, motor tilting	O yes / C yes			
4, comp. tilting	O yes / C yes			
5, 1.bend. comp.	O weak / C weak	O weak / C weak	O yes / C yes	O yes / C yes
6, 2.bend. comp.	O weak / C weak	O weak / C weak	O yes / C yes	O yes / C yes
7, 2.bend. comp.*	O weak / C weak	O weak / C weak	O yes / C yes	O yes / C no
8, 3.bend. comp.	O weak / C weak	O weak / C no	O yes / C yes	O no / C yes
9, 1.bend. motor	O yes / C yes	C yes / O yes	O yes / C yes	O no / C yes
10, 3.bend.comp.+	O yes / C yes			
11, 2.bend.motor	O yes / C yes	O yes / C no	O weak / C weak	O weak / C weak

* Quill shaft has one more node compared to 6.

+ Quill shaft has one more node compared to 8.

O = Observability

C = Commandability

Table 2. Necessary and Realized Compressor Bearing Characteristics at the Bending Mode Frequency.

	according to figure 5	according to figure 6	DE bearing	NDE bearing
k [N/m]	10^7	$2 \cdot 10^7$	$1.66 \cdot 10^7$	$2.3 \cdot 10^7$
d [Ns/m]	8000	8000	$2.44 \cdot 10^3$	$1.4 \cdot 10^4$
A [N/m]	$1.55 \cdot 10^7$	$2.4 \cdot 10^7$	$1.7 \cdot 10^7$	$3.2 \cdot 10^7$
ϕ [degree]	50	33	12.5	42

Table 3. Frequencies and Damping Ratios of the Closed Loop System

mode	$f_{\text{calculated}}$ [Hz]	$D_{\text{calculated}}$ [%]	f_{measured} [Hz]	$ \Delta f/f_{\text{measured}} $
1, motor parallel	45.5	31.3	45	0.0 %
2, comp.parallel	68.1	23.2	68	0.0 %
3, motor tilting	102.1	27.5	102	0.0 %
4, comp. tilting	124.7	34.1	125	0.2 %
5, 1.bend. comp.	243.2	11.6	240	1.3 %
6, 2.bend.comp.	389.5	1.9	405	3.8 %
7, 2.bend.comp.*	514.8	0.1	540	4.7 %
8, 3.bend.comp.	754.7	-1.8(unstable)	840	10.1 %
9, 1.bend.motor	1038.7	0.5		
10, 3.bend.comp.+	1158.4	0.2	1180	1.8 %
11, 2.bend.motor	1470.9	-1.0(unstable)	1350	9.0 %

* Quill shaft has one more node compared to 6.

+ Quill shaft has one more node compared to 8.

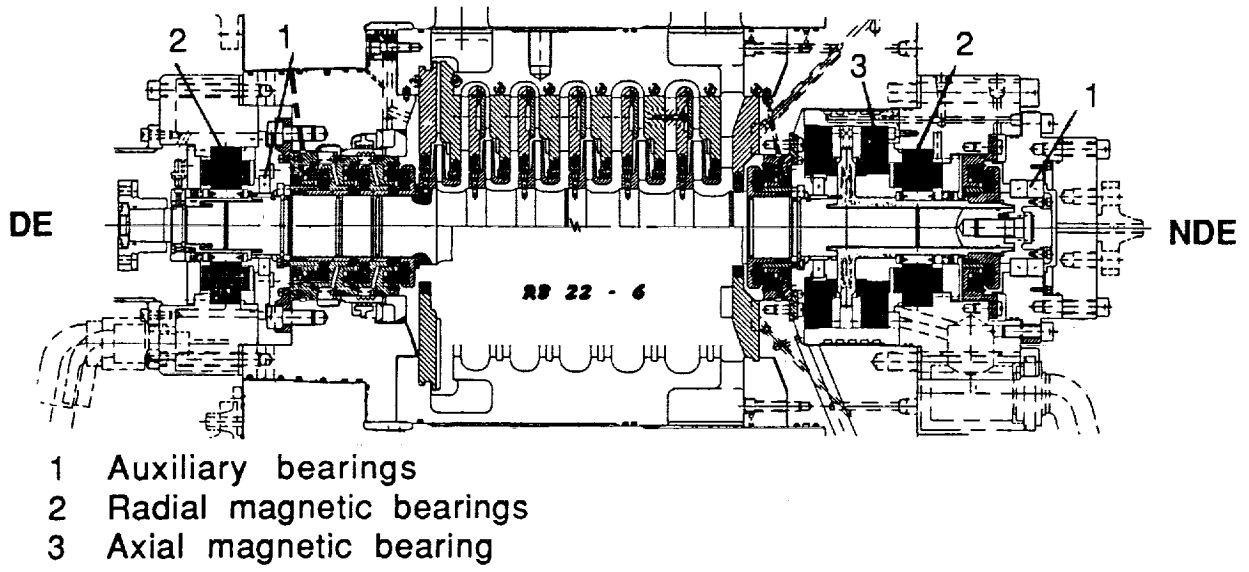


Figure 1. Cross section of the compressor.

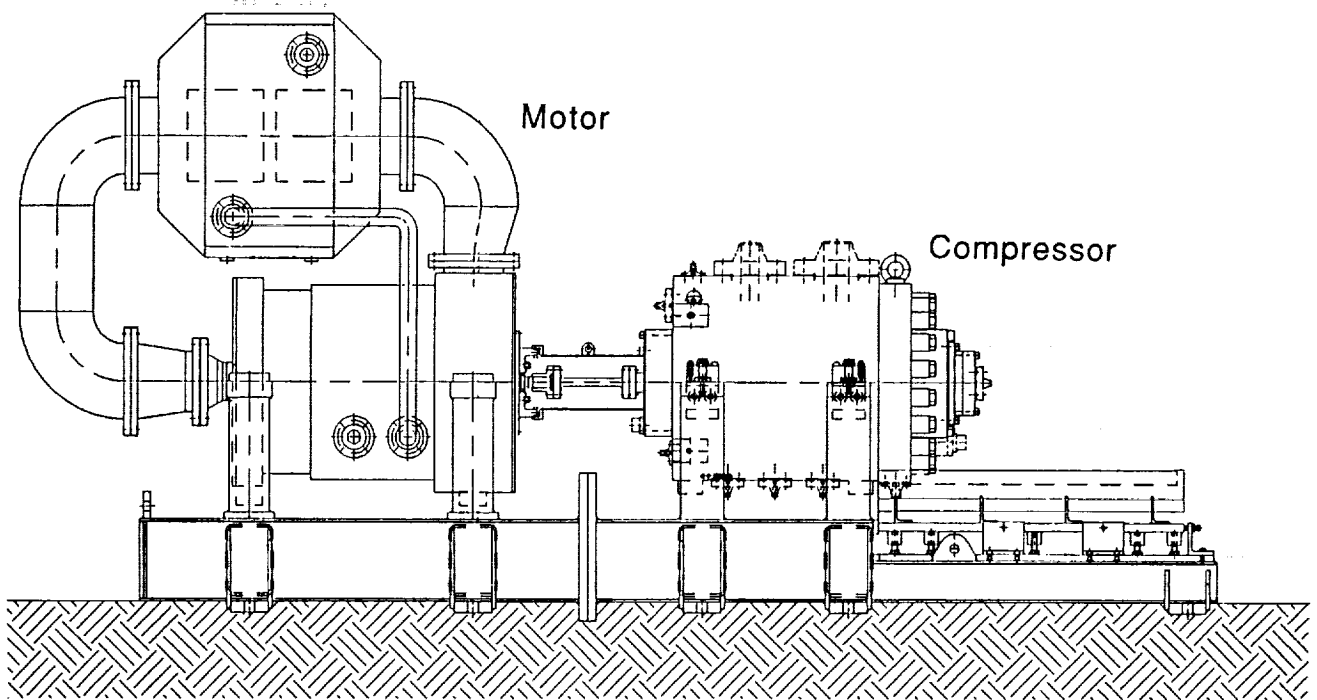


Figure 2. Arrangement of the motor compressor unit.

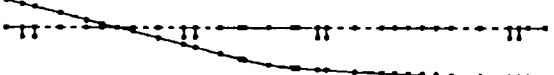
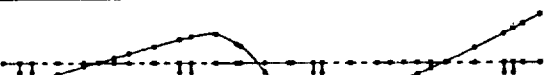
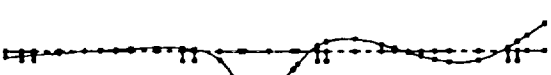
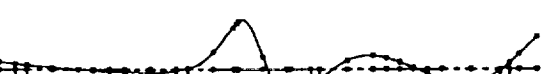
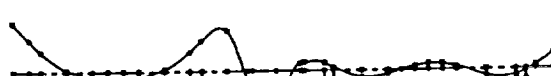
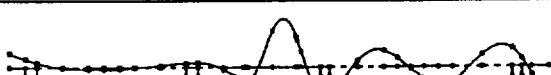
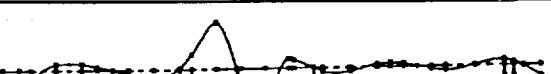
Mode Shape	Number, Frequency
	1, 15.0Hz
	2, 22.4Hz
	3, 29.2Hz
	4, 76.4Hz
	5, 220.9Hz
	6, 378.9Hz
	7, 515.4Hz
	8, 787.1Hz
	9, 994.9Hz
	10, 1162.5Hz
	11, 1463.0Hz

Figure 3. Modes of the coupled shaft supported on soft springs ($k=10^6\text{N/m}$).

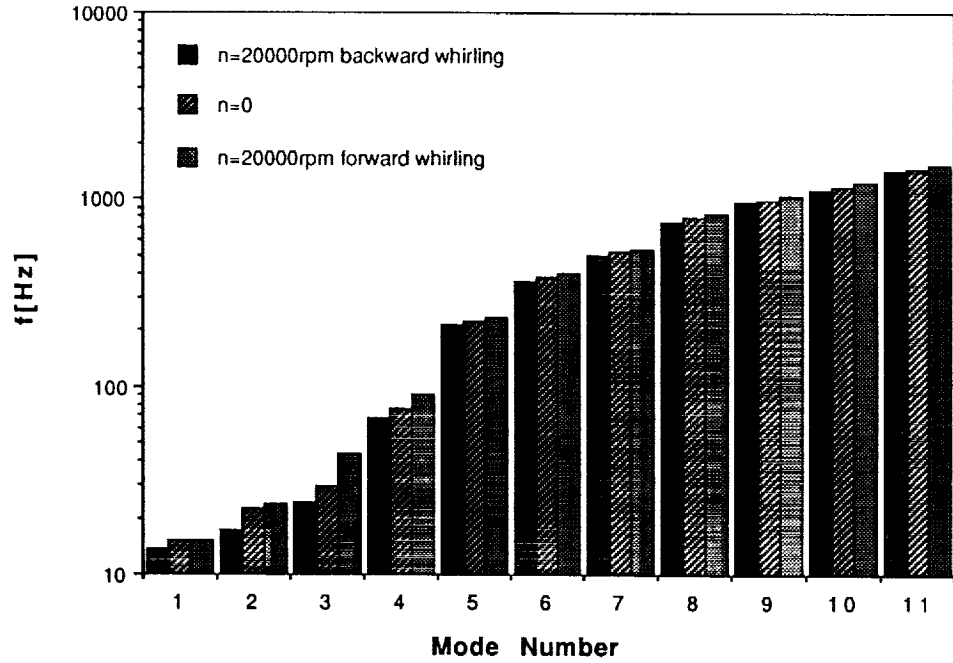


Figure 4. Natural frequencies of the shaft at standstill and full speed.

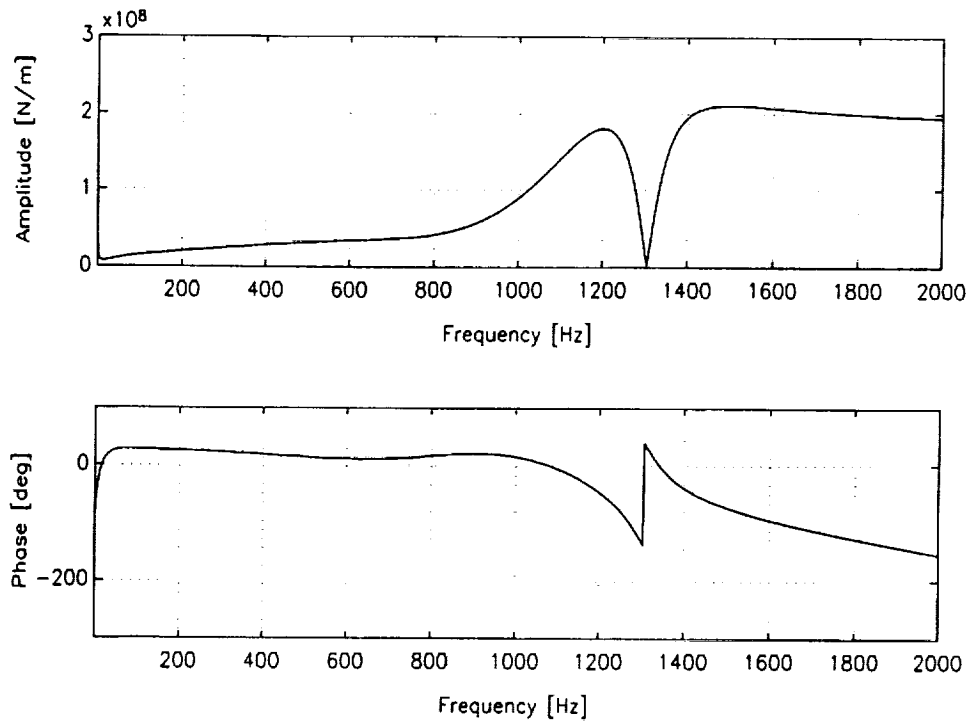


Figure 5. Transfer function of the motor magnetic bearings.

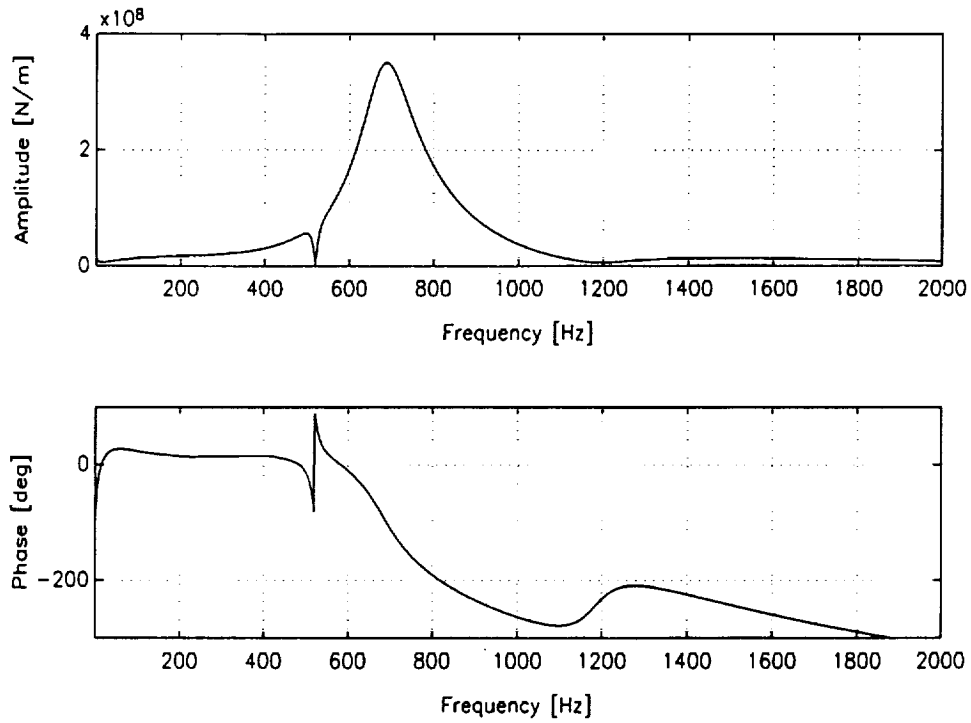


Figure 6. Transfer function of the DE compressor magnetic bearing.

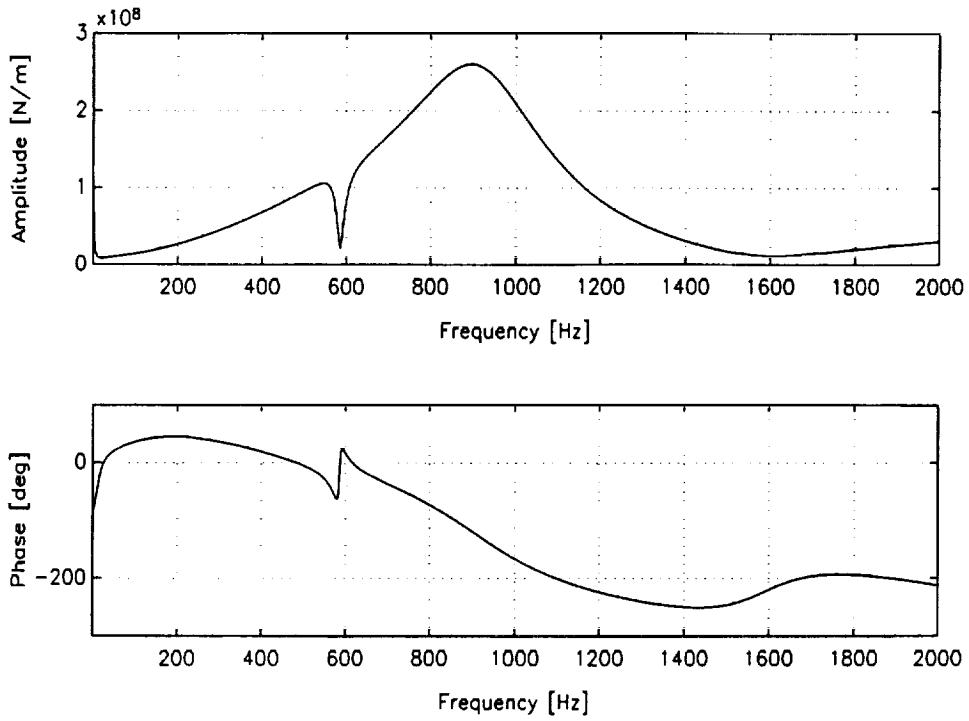


Figure 7. Transfer function of the NDE compressor magnetic bearing.

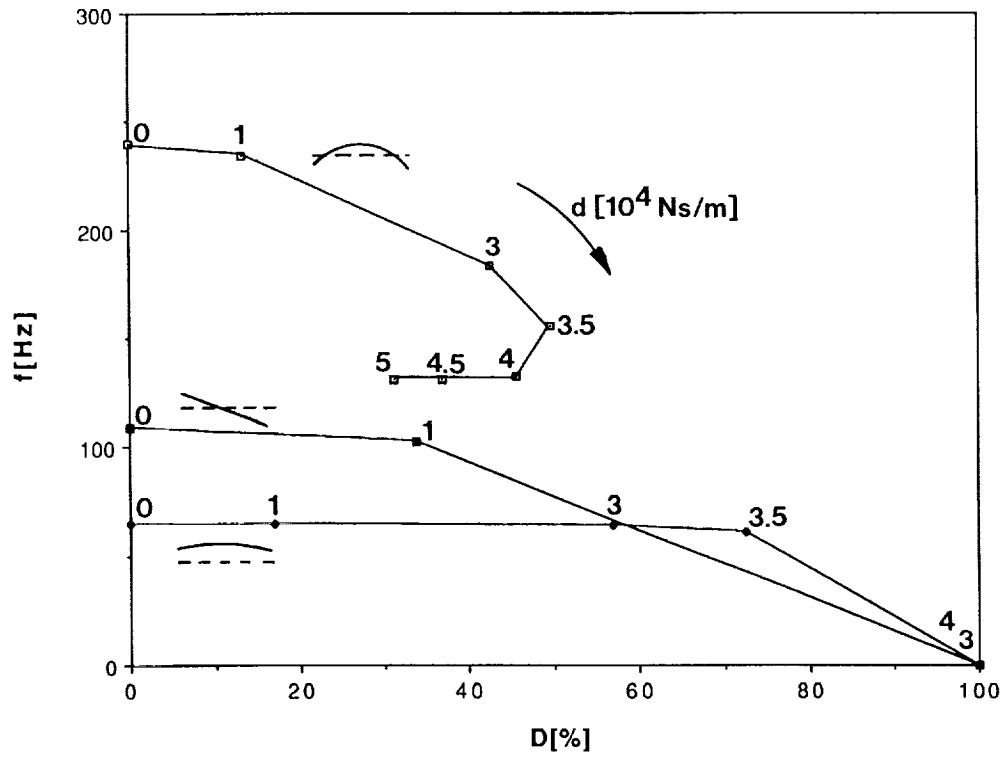


Figure 8. Eigenvalues of the compressor rotor as a function of the bearing damping for a bearing stiffness of 10^7 N/m.

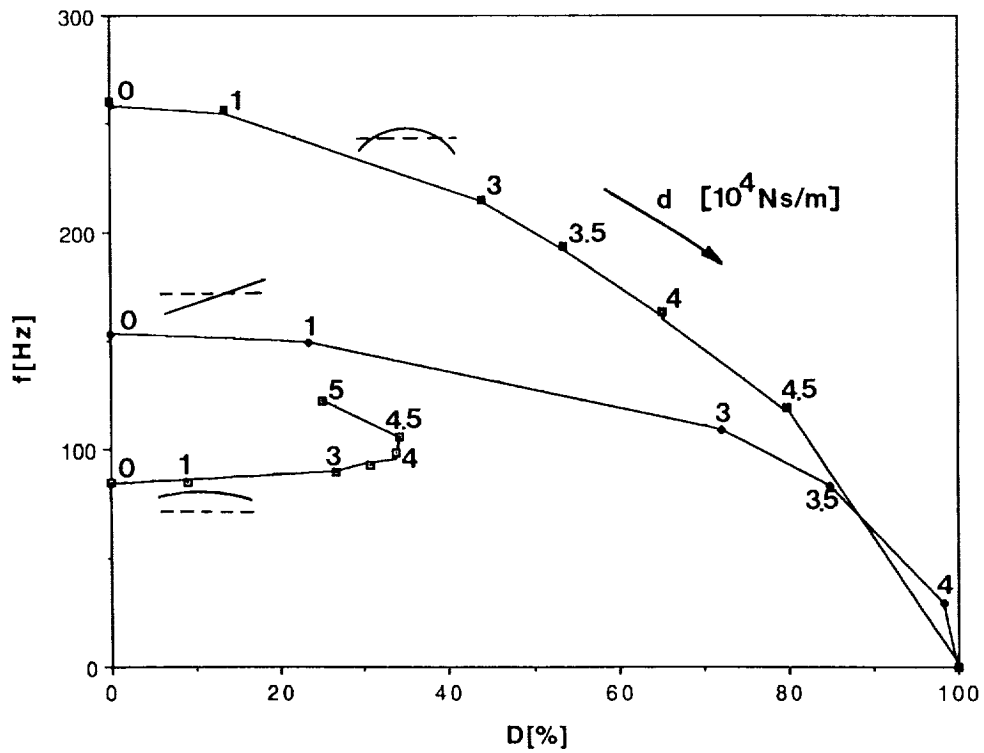


Figure 9. Eigenvalues of the compressor rotor as a function of the bearing damping for a bearing stiffness of $2.0 \cdot 10^7$ N/m.

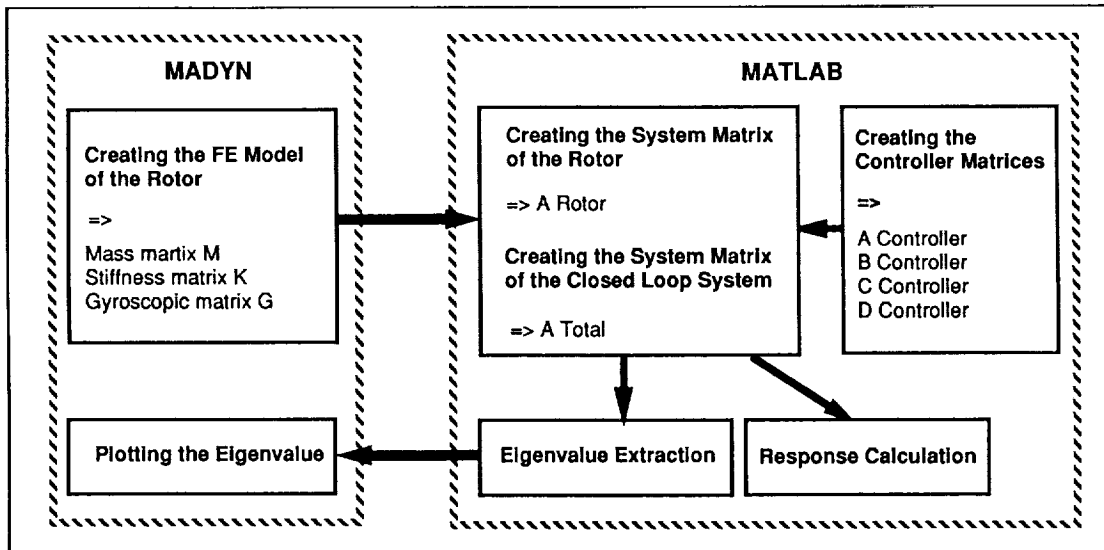


Figure 10. Procedure for closed loop calculations.

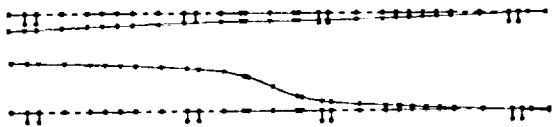
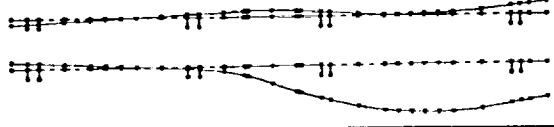
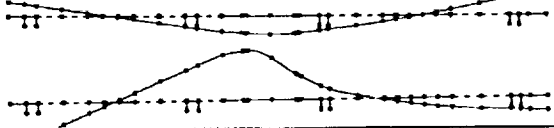
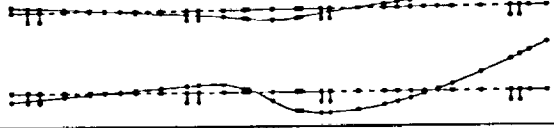
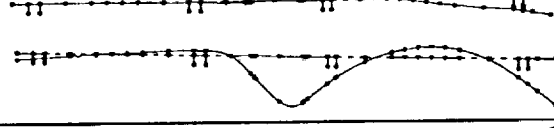
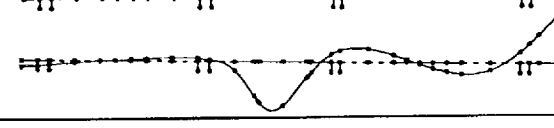
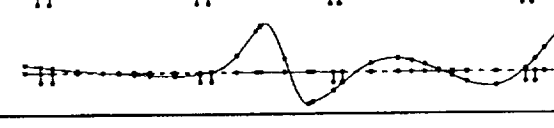
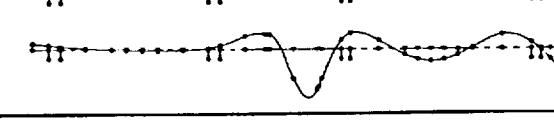
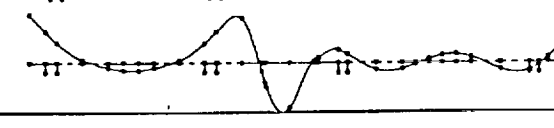
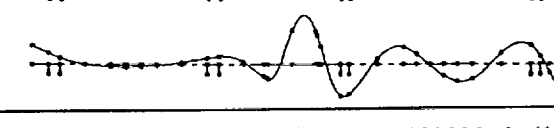
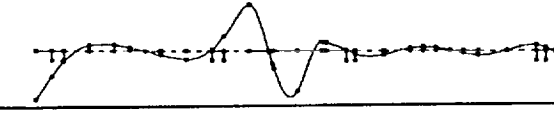
Mode Shape		Number, Freq., Damp.Ratio
Im Re		1, 45.5Hz, 31.3%
Im Re		2, 68.1Hz, 23.2%
Im Re		3, 102.1Hz, 27.5%
Im Re		4, 124.7Hz, 34.1%
Im Re		5, 243.2Hz, 11.6%
Im Re		6, 389.5Hz, 1.9%
Im Re		7, 514.8Hz, 0.1%
Im Re		8, 754.7Hz, -1.8%
Im Re		9, 1038.7Hz, 0.5%
Im Re		10, 1158.4Hz, 0.2%
Im Re		11, 1470.9Hz, -1.0%

Figure 11. Rotor modes of the closed loop system.

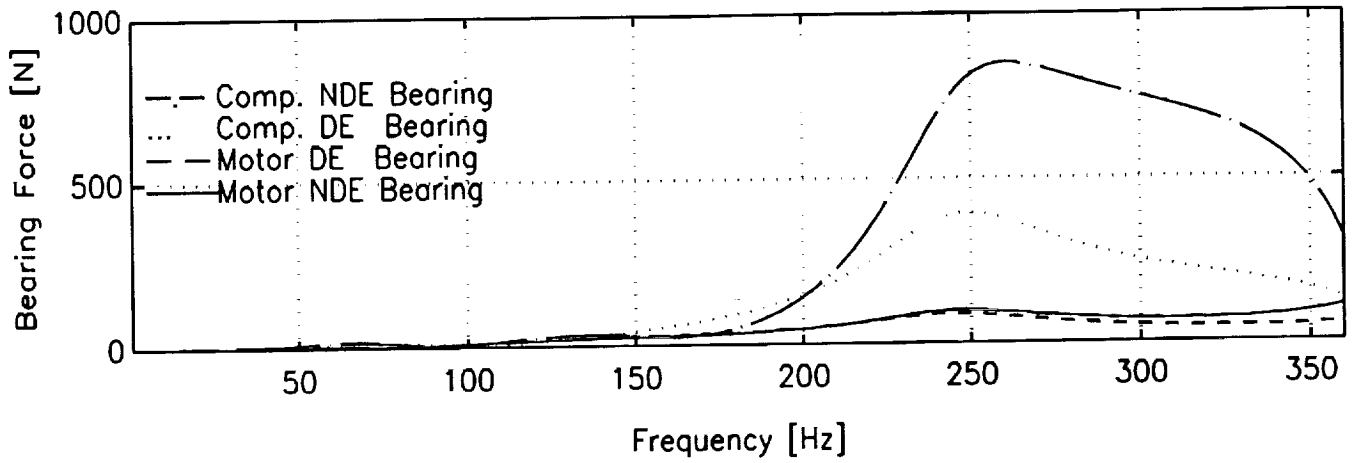


Figure 12. Bearing responses to a parallel unbalance (G2.5) in the compressor.

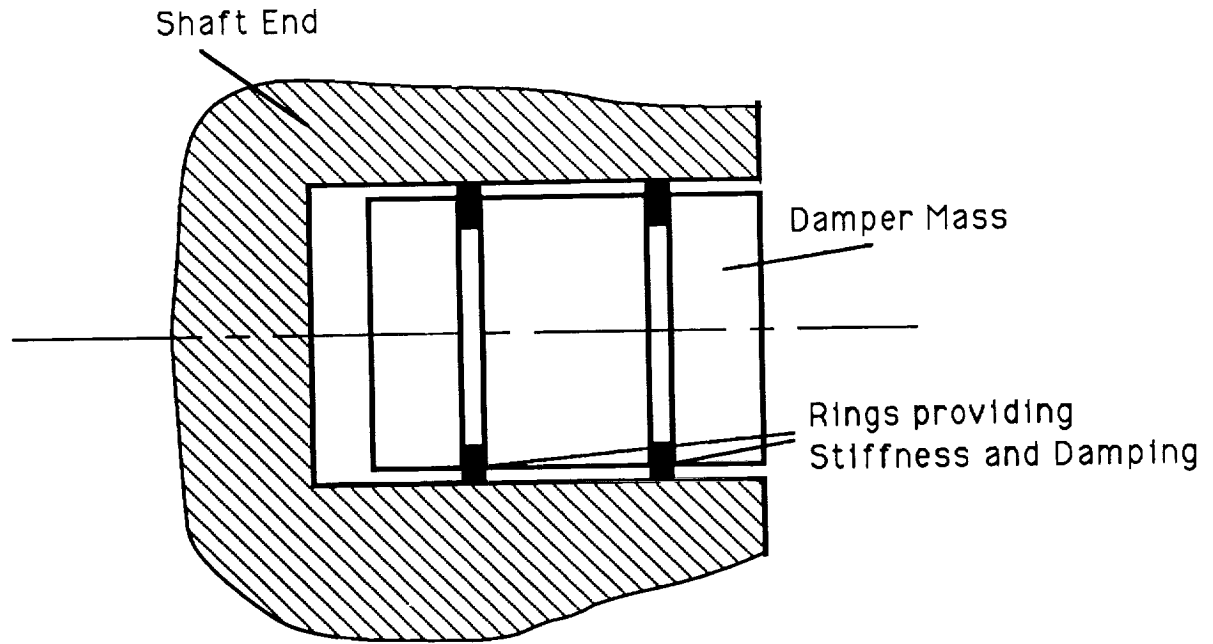


Figure 13. Sketch of the mechanical damper.

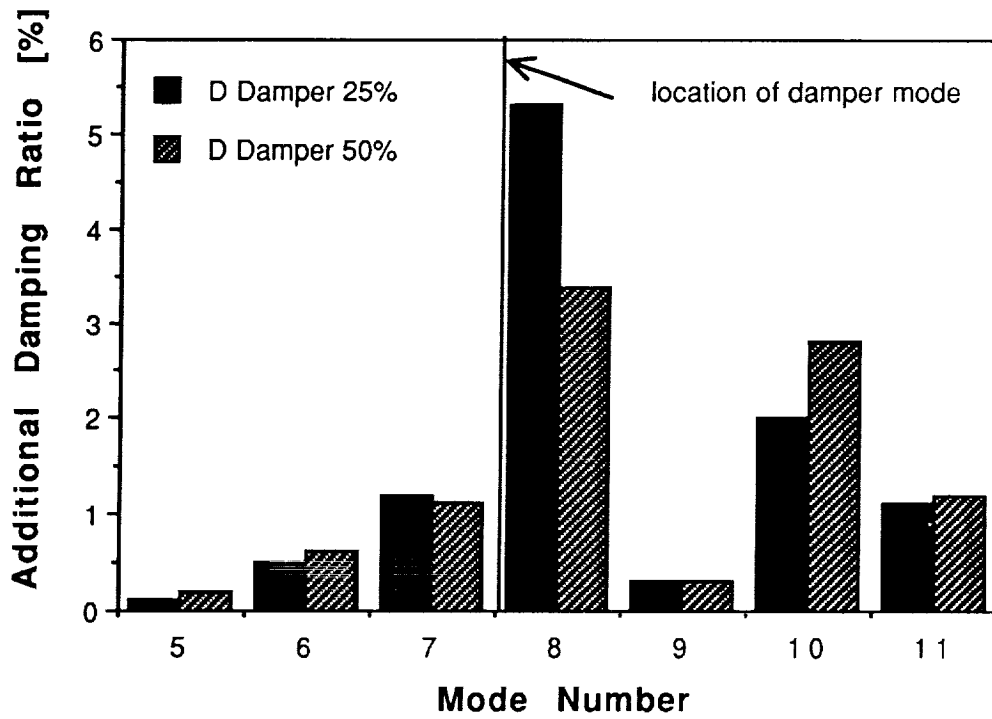
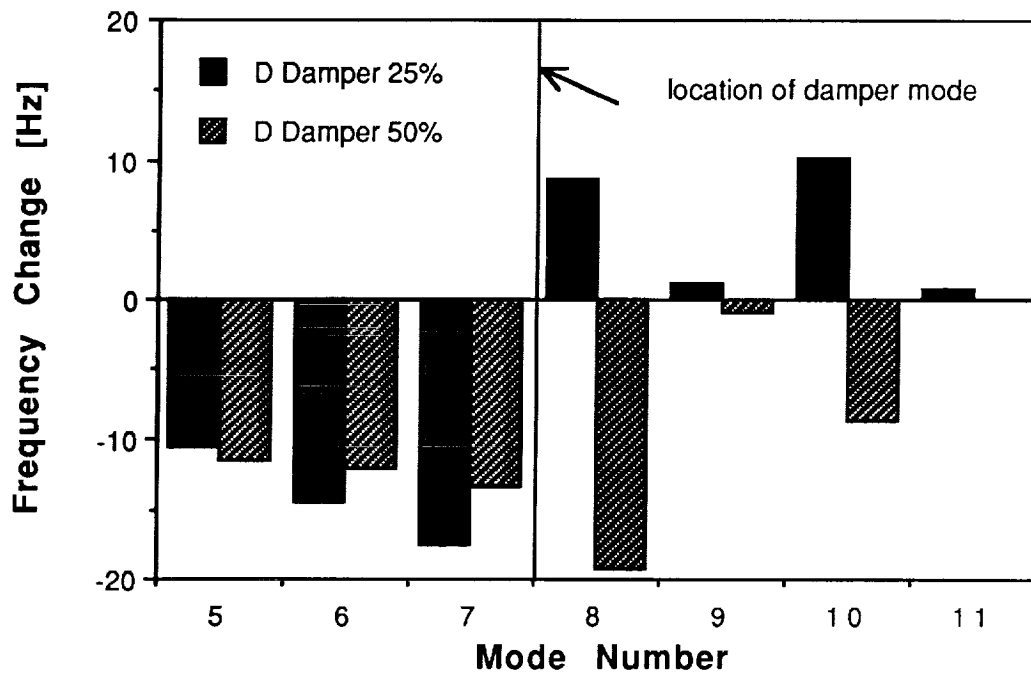


Figure 14. Effect of a mechanical damper on the rotor modes.

omit

Session 10a – Controls

Chairman: Alexander V. Kuzin
Moscow Aviation Technological Institute

